Please cite this article in press as: Küry et al., De Novo Disruption of the Proteasome Regulatory Subunit *PSMD12* Causes a Syndromic Neurodevelopmental Disorder, The American Journal of Human Genetics (2017), http://dx.doi.org/10.1016/j.ajhg.2017.01.003

REPORT

De Novo Disruption of the Proteasome Regulatory Subunit *PSMD12* Causes a Syndromic Neurodevelopmental Disorder

Sébastien Küry,[1] Thomas Besnard,[1] Frédéric Ebstein,[2] Tahir N. Khan,[3] Tomasz Gambin,[4,5,6] Jessica Douglas,[7] Carlos A. Bacino,[4,8] Stephan J. Sanders,[9] Andrea Lehmann,[2] Xénia Latypova,[1] Kamal Khan,[3] Mathilde Pacault,[1] Stephanie Sacharow,[7] Kimberly Glaser,[10] Eric Bieth,[11] Laurence Perrin-Sabourin,[12] Marie-Line Jacquemont,[13] Megan T. Cho,[14] Elizabeth Roeder,[4,15] Anne-Sophie Denommé-Pichon,[16] Kristin G. Monaghan,[14] Bo Yuan,[4,8] Fan Xia,[4,8] Sylvain Simon,[17,18,19] Dominique Bonneau,[16,20] Philippe Parent,[21] Brigitte Gilbert-Dussardier,[22,23] Sylvie Odent,[24,25] Annick Toutain,[26,27] Laurent Pasquier,[24,25] Deborah Barbouth,[10] Chad A. Shaw,[4,8] Ankita Patel,[4,8] Janice L. Smith,[4,8] Weimin Bi,[4,8] Sébastien Schmitt,[1] Wallid Deb,[1] Mathilde Nizon,[1] Sandra Mercier,[1] Marie Vincent,[1] Caroline Rooryck,[28] Valérie Malan,[29] Ignacio Briceño,[30] Alberto Gómez,[30] Kimberly M. Nugent,[15] James B. Gibson,[31] Benjamin Cogné,[1] James R. Lupski,[4,32,33] Holly A.F. Stessman,[34] Evan E. Eichler,[34,35] Kyle Retterer,[14] Yaping Yang,[4,8] Richard Redon,[36,37] Nicholas Katsanis,[3,38] Jill A. Rosenfeld,[4] Peter-Michael Kloetzel,[2] Christelle Golzio,[3] Stéphane Bézieau,[1,17] Paweł Stankiewicz,[4,8,39,40,*] and Bertrand Isidor[1,40,*]

Degradation of proteins by the ubiquitin-proteasome system (UPS) is an essential biological process in the development of eukaryotic organisms. Dysregulation of this mechanism leads to numerous human neurodegenerative or neurodevelopmental disorders. Through a multi-center collaboration, we identified six de novo genomic deletions and four de novo point mutations involving *PSMD12*, encoding the non-ATPase subunit PSMD12 (aka RPN5) of the 19S regulator of 26S proteasome complex, in unrelated individuals with intellectual disability, congenital malformations, ophthalmologic anomalies, feeding difficulties, deafness, and subtle dysmorphic facial features. We observed reduced PSMD12 levels and an accumulation of ubiquitinated proteins without any impairment of proteasome catalytic activity. Our *PSMD12* loss-of-function zebrafish CRISPR/Cas9 model exhibited microcephaly, decreased convolution of the renal tubules, and abnormal craniofacial morphology. Our data support the biological importance of PSMD12 as a scaffolding subunit in proteasome function during development and neurogenesis in particular; they enable the definition of a neurodevelopmental disorder due to *PSMD12* variants, expanding the phenotypic spectrum of UPS-dependent disorders.

Proteolysis by the ubiquitin-proteasome system (UPS) is a tightly regulated biological process in eukaryotic cells and is crucial for their homeostasis, signaling, and fate determination.[1–3] Proteins subjected to degradation are typically marked by polyubiquitin chains to be hydrolyzed in a precise, rapid, timely, and ATP-dependent manner by the 19S regulatory subunit of the 26S proteasome.[3–6] UPS-dependent degradation essentially contributes to proteostasis and plays a key role in neuronal development and function[7,8] by regulating synaptic plasticity,[9,10]

[1]Service de Génétique Médicale, CHU de Nantes, 9 quai Moncousu, 44093 Nantes Cedex 1, France; [2]Institute of Biochemistry, Charité Universitätsmedizin Berlin, Charité Platz 1/Virchowweg 6, 10117 Berlin, Germany; [3]Center for Human Disease Modeling, Duke University Medical Center, Durham, NC 27710, USA; [4]Department of Molecular and Human Genetics, Baylor College of Medicine, Houston, TX 77030, USA; [5]Institute of Computer Science, Warsaw University of Technology, Warsaw 00-661, Poland; [6]Department of Medical Genetics, Institute of Mother and Child, Warsaw 01-211, Poland; [7]Division of Genetics and Genomics, Boston Children's Hospital and Harvard Medical School, Boston, MA 02115, USA; [8]Baylor Genetics, Houston TX, 77030, USA; [9]Department of Psychiatry, Weill Institute for Neurosciences, University of California, San Francisco, San Francisco, CA 94158, USA; [10]Dr. John T. Macdonald Foundation Department of Human Genetics, Miller School of Medicine, University of Miami, Miami, FL 33136, USA; [11]Service de Génétique Médicale, Hôpital Purpan, CHU de Toulouse, 31059 Toulouse, France; [12]Fédération de Génétique, Hôpital Robert Debré, Assistance Publique – Hôpitaux de Paris, 75935 Paris Cedex 19, France; [13]Génétique Médicale, CHU de La Réunion, 97448 Saint Pierre, La Réunion, France; [14]GeneDx, Gaithersburg, MD 20877, USA; [15]Department of Pediatrics, Baylor College of Medicine, San Antonio, TX 78207, USA; [16]Département de Biochimie et Génétique, CHU d'Angers, 49933 Angers Cedex 9, France; [17]Centre de Recherche en Cancérologie et Immunologie Nantes-Angers, INSERM, Université d'Angers et Université de Nantes, 44007 Nantes, France; [18]LabEx "Immunotherapy, Graft, Oncology," 44093 Nantes, France; [19]Department of Dermato-cancerology, CHU de Nantes, 44093 Nantes, France; [20]INSERM UMR 1083, CNRS UMR 6214, 49933 Angers Cedex 9, France; [21]Génétique Médicale, CHRU de Brest, 29609 Brest, France; [22]Service de Génétique, CHU de Poitiers, BP 577, 86021 Poitiers, France; [23]Equipe d'Accueil 3808, Université de Poitiers, 86022 Poitiers Cedex, France; [24]Service de Génétique Clinique, Centre Hospitalier Universitaire de Rennes, 35203 Rennes, France; [25]CNRS UMR 6290, Université de Rennes 1, 2 Avenue du Professeur Léon Bernard, 35043 Rennes, France; [26]Service de Génétique, CHU de Tours, 2 Boulevard Tonnellé, 37044 Tours, France; [27]INSERM UMR U930, Faculté de Médecine, Université François Rabelais, 37044 Tours, France; [28]Service de Génétique Médicale, CHU de Bordeaux, 33076 Bordeaux, France; [29]Service d'Histologie-Embryologie-Cytogénétique, Hôpital Necker-Enfants Malades, Assistance Publique – Hôpitaux de Paris, 75015 Paris, France; [30]Instituto de Genética Humana, Facultad de Medicina, Pontificia Universidad Javeriana, 110231 Bogotá, Colombia; [31]Clinical and Metabolic Genetics, 'Specially for Children, Austin, TX 78723, USA; [32]Department of Pediatrics, Texas Children's Hospital, Houston, TX 77030, USA; [33]Human Genome Sequencing Center, Baylor College of Medicine, Houston, TX 77030, USA; [34]Department of Genome Sciences, University of Washington School of Medicine, Seattle, WA 98195, USA; [35]Howard Hughes Medical Institute, Seattle, WA 98195, USA; [36]INSERM, CNRS, l'Institut du Thorax, Université de Nantes, 44007 Nantes, France; [37]L'Institut du Thorax, CHU de Nantes, 44093 Nantes, France; [38]Department of Cell Biology, Duke University Medical Center, Durham, NC 27710, USA; [39]Institute of Mother and Child, Warsaw 01-211, Poland
[40]These authors equally contributed to this work
*Correspondence: pawels@bcm.edu (P.S.), bertrand.isidor@chu-nantes.fr (B.I.)
http://dx.doi.org/10.1016/j.ajhg.2017.01.003.

Table 1. Clinical Features of the Subjects with De Novo Point Mutations and CNV Deletions Involving *PSMD12*

	Subject 1	Subject 2	Subject 3	Subject 4	Subject 5	Subject 6	Subject 7	Subject 8	Subject 9	Subject 10
Center of enrollment	HUGODIMS	BCH	SSC	BG	BG	BG	CHU de Toulouse	CHU de la Réunion	BG	BG
PSMD12 variant[a]	c.367C>T (p.Arg123*)	c.1274 T>G (p.Leu425*)	c.601C>T (p.Arg201*)	c.909−2A>G (p.?)	deletion	deletion	deletion	deletion	deletion	deletion
Size of deletion (Mb)	–	–	–	–	1.37	4.06	1.46	1.24	0.84	0.62 (complex)
Deletion proximal breakpoints[b]	–	–	–	–	64,585,784–64,598,722	62,280,810–62,289,975	64,529,282–64,590,936	64,461,987–64,529,223	65,319,589	65,090,765
Deletion distal breakpoints[b]	–	–	–	–	65,972,166–66,162,742	66,352,008–66,398,204	65,955,949–65,989,022	65,720,329–65,766,756	66,162,742	65,711,757
Gender	male	male	male	male	female	male	male	female	female	female
Age at assessment	8 y, 4 m	10 y, 7 m	14 y, 8 m	14 y, 10 m	21 m	3 y, 6 m	13 y, 2 m	5 y, 11 m	4 y, 6 m	9 y
Weight (g) at birth (SD)	2,500 (−2)	2,466 (−2)	3,033 (−0.84)	3,200 (−0.5)	ND	2,390 (−2.2)	1,570 (−4)	2,590 (−1.5)	1,900 (−2.9)	2,100 (−2.5)
Length (cm) at birth (SD)	46 (−2)	43 (−3.5)	48.3 (−0.70)	50 (mean)	ND	47 (−1.5)	44 (−3)	43.5 (−3)	43.2 (−2.8)	46 (−1.55)
OFC (cm) at birth (SD)	36 (+1)	32 (−2)	34.9 (−0.44)	ND	ND	32 (−2)	33.5 (−1)	32 (−2)	30 (−3.3)	ND
Weight (kg) at assessment (SD)	25 (−0.5)	28.6 (−1)	61.7 (+0.60)	42.4 (−1)	ND	11.3 (−2.64)	31 (−2)	16.8 (−1.37)	ND (3rd percentile)	40 (+1.36)
Length (cm) at assessment (SD)	120 (−1)	129.8 (−1.7)	173 (+0.84)	163 (mean)	ND	91 (−2.2)	134 (−2.5)	103.5 (−2.07)	ND (10th–25th percentile)	140 (+1.10)
OFC (cm) at assessment (SD)	52.5 (−0.5)	52 (−1)	57 (+1.48)	ND	ND, microcephaly	47.6 (−1.6)	51.5 (−2)	50 (−0.57)	ND (5th–10th percentile)	55 (+2.32)
Neurological Abnormalities										
Intellectual disability	+	+	+	+	+	+	+	+	+	+
Motor delay	+	+	−	−	+	+	+	−	+	+
Speech delay	+	+	+	−	+	+	+	+	+	+
Abnormal behavior	+	+	+	+	−	ND	+	+	ND	+
Seizures	−	+	−	+	−	−	−	−	−	+
Hypotonia	+	−	ND	+	−	+	+	−	+	+
Deafness	+	+	−	−	−	+	−	−	−	−
Feeding difficulties	+	+	−	−	−	+	+	−	+	−
Brain MRI	normal	normal	ND	abnormal	ND	abnormal	normal	normal	ND	normal
Congenital Malformations										
Cardiac	+	+	+	−	+	+	−	−	−	−
Renal	+	+	−	ND	+	+	−	−	+	+

(*Continued on next page*)

Table 1. *Continued*

	Subject 1	Subject 2	Subject 3	Subject 4	Subject 5	Subject 6	Subject 7	Subject 8	Subject 9	Subject 10
Genital	+	+	+	+	–	+	–	–	–	+
Skeletal	+	+	–	–	–	+	+	–	+	–
Other	–	+	–	–	–	–	–	–	–	–
Craniofacial Abnormalities										
Ophthalmological	+	+	ND	+	+	+	+	–	+	+
Ears	+	+	ND	+	–	+	–	+	+	+
(Micro)retrognathia	+	–	ND	–	+	–	+	–	+	–
Other	–	–	ND	+	+	+	+	+	+	+

More comprehensive information regarding clinical features is cataloged in Table S1. Abbreviations are as follows: y, years; m, months; ND, not determined; SD, standard deviation; OFC, occipito-frontal circumference; MRI, magnetic resonance imaging; CHU, Centre Hospitalier Universitaire; BCH, Boston Children's Hospital; BG, Baylor Genetics Laboratories; and SSC, Simons Simplex Collection.
[a]For SNVs: HGVS nomenclature version 2.0 according to mRNA reference sequence GenBank: NM_002816.3. Nucleotide numbering uses 1 as the initiation codon and +1 as the A of the ATG translation initiation codon in the reference sequence.
[b]Human genome reference: UCSC Genome Browser hg19.

neurotransmitter release via intracellular trafficking,[11,12] and morphogenesis of axons, dendrites, and dendritic spines.[7] Neurons are therefore highly vulnerable to UPS dysfunction, as evidenced by a wide spectrum of neurodegenerative proteinopathies, including polyglutamine disorders (e.g., spinal bulbar muscular atrophy [MIM: 313200] and Huntington disease [MIM: 143100]), Alzheimer disease (MIM: 104300), Parkinson disease (MIM: 168600), and amyotrophic lateral sclerosis (MIM:105400).[13,14] Impairment of UPS activity can also result in neurodevelopmental delay, as exemplified by alterations of ubiquitin ligase genes *UBE3A* (MIM: 601623; associated with Angelman syndrome [MIM: 105830]),[15] *UBE3B* (MIM: 608047; associated with Kaufman oculocerebrofacial syndrome [MIM: 244450]),[16] and *HUWE1* (MIM: 300697; associated with X-linked Turner-type syndromic mental retardation [MIM: 300706])[17] and deubiquitinating enzyme genes *USP7* (MIM: 602519; associated with chromosome 16p13.2 deletion syndrome [MIM: 616863])[18] and *USP9X* (MIM: 300072; associated with mental retardation, X-linked 99 [MIM: 300919] and mental retardation, X-linked 99, syndromic, female-restricted [MIM: 300968]).[19]

Herein, we report ten unrelated individuals exhibiting a syndromic form of intellectual disability (ID) due to copy-number variant (CNV) deletions or single-nucleotide variants (SNVs) involving *PSMD12* (MIM: 604450), encoding the 456-amino-acid non-ATPase subunit PSMD12 (or RPN5) of the 26S proteasome. The compilation of this case series resulted from an international collaborative effort among Western France consortium HUGODIMS (Hôpitaux Universitaires du Grand Ouest pour l'Exploration par Approche Exome des Causes Moléculaires de Déficience Intellectuelle Isolée ou Syndromique Modérée à Sévère), Baylor Genetics Laboratories (BG), Boston Children's Hospital and GeneDX, the Simons Simplex Collection, Centre Hospitalier Universitaire (CHU) de La Réunion and Hôpital Robert Debré, and CHU de Toulouse. It was also partly facilitated by the web-based tools GeneMatcher[20] and DECIPHER.[21]

This study was approved by both the CHU de Nantes ethics committee (comité consultatif sur le traitement de l'information en matière de recherche no. 14.556) and the Baylor College of Medicine institutional review board. All participants were clinically assessed by at least one expert clinical geneticist from one of the participating centers. Written informed consent was obtained from all study participants. The main clinical features of our cohort are summarized in Table 1. More detailed clinical information for all subjects is provided in the Supplemental Note and Table S1, and corresponding Human Phenotype Ontology terms are reported in Tables S2 and S3.

Three de novo nonsense SNVs in *PSMD12* (GenBank: NM_002816.3)—c.367C>T (p.Arg123*) in subject 1, c.1274T>G (p.Leu425*) in subject 2, and c.601C>T (p.Arg201*) in subject 3—were found by subject-parent trio-based whole-exome sequencing. The protocols used

by each participating center have been detailed elsewhere.[22–24] These three variants were confirmed by Sanger sequencing. They were unique events observed in our in-house database of about 350 exomes (including 75 trios from families with simplex ID) for subject 1 (HUGODIMS and CHU de Nantes); in over 40,000 exomes, including 2,300 trios with various developmental disorders, for subject 2 (Boston Children's Hospital and GeneDX); and in 2,500 trios with autism spectrum disorders for subject 3 (Simons Simplex Collection) (Figure S2). These three variants are also absent in public variant databases (dbSNP138, 1000 Genomes, NHLBI GO Exome Sequencing Project, and the Exome Aggregation Consortium [ExAC] Browser). In addition, a query of over 7,000 clinical exomes in the BG database, according to the previously defined clinical diagnostics protocol,[25,26] revealed de novo splicing variant c.909−2A>G (p.?) in subject 4 (Figure S2). Differently sized de novo CNV deletions on 17q24.2 were found in four unrelated individuals (subjects 5, 6, 9, and 10) among 59,092 subjects referred for chromosomal microarray analysis (CMA) at BG between January 4, 2004, and May 6, 2016; they were tested with customized exon-targeted oligonucleotide arrays (OLIGO V8, V9, and V10) designed at BG,[27,28] which cover more than 4,800 known or candidate disease genes with exon-level resolution. The two remaining individuals, subjects 7 and 8, were recruited via DECIPHER (accession numbers 286468 and 300694). The largest CNV deletion in the series is about 4 Mb in size and includes *PSMD12* and 27 other genes, whereas the smallest deletion, 0.62 Mb, encompasses *PSMD12*, *PITPNC1* (MIM: 605134), and a portion of *HELZ* (MIM: 606699) (Figure 1 and Table S4). Minimal and maximal coordinates of the CNV deletions are indicated in Tables 1 and S1. In the BG in-house database, apparently similarly sized ~270 kb 17q24.2 duplication CNVs (chr17: 65,081,882–65,388,883 and 65,120,043–65,458,702; UCSC Genome Browser hg19), involving the entire *PSMD12*, were observed in three unrelated families. In two of these families, the duplication was inherited from the reportedly asymptomatic parents. Moreover, in one of these families, a pathogenic de novo CNV deletion in chromosomal region 2p14p15, explaining the subject's phenotype, was detected. Thus, this duplication most likely represents a rare nonpathogenic CNV. No constitutive de novo small duplication was recorded in DECIPHER[21] or in the Database of Genomic Variants.[29]

All subjects from the case series exhibited developmental delay (DD) or ID (n = 10) and had variable dysmorphic features, among which low-set ears (n = 6), hypertelorism (n = 5), and retrognathia or microretrognathia (n = 4) were the most frequent. All but one individual had additional neurological features, including abnormal behavior (n = 7, mostly autistic features or hyperactivity), hypotonia (n = 6), or epilepsy (n = 3, including seizure disorder, reflex seizures, and tonic convulsion). Additionally, two of six subjects had abnormalities detected on brain imaging (pineal cyst [n = 2], cerebral atrophy, and periventricular hypomyelination [n = 1]). Nine subjects had other congenital anomalies, including an atrio- or ventriculoseptal defect, patent ductus arteriosus, a single or dysplastic kidney, hydronephrosis, or genital anomalies (hypospadias or cryptorchidism). Five subjects had a history of feeding difficulties evident already in the neonatal period and associated with growth failure in four cases. Three subjects required gastrostomy feeding tubes. Seven subjects also had ophthalmologic anomalies, including strabismus, vision loss, and coloboma. Five subjects had skeletal abnormalities, including bilateral syndactyly of the second and third toes (n = 3) and thumb agenesis or hypoplasia (n = 2). Microcephaly was noted in five subjects, whereas macrocephaly was noted in one subject.

The 26S proteasome is a high-molecular-weight multisubunit proteinase complex of nearly 2.5 MDa whose structure, assembly, and functions are highly conserved across eukaryotes[1,5,30] (Figure S3). It is composed of two functionally distinct subcomplexes and responsible for the ATP-dependent degradation of poly-ubiquitinated proteins. The 19S regulatory particle (~900 kDa) binds and unfolds the ubiquitinated substrates, and the 20S proteolytic core (~700 kDa) is responsible for the hydrolysis of the substrate proteins.[31,32] The 19S particle, attached at either or both ends of the 20S particle, consists of two sub-complexes, the base and the lid. The base is composed of six ATPases (regulatory particle triple A proteins RPT1–RPT6), two large organizing subunits (regulatory particle non-ATPases 1 [RPN1] and 2 [RPN2]), and two ubiquitin receptors (RPN10 and RPN13).[1,31–34] The lid is formed from the deubiquitylating enzyme RPN11 and eight non-ATPase subunits (RPN3, RPN5–RPN9, RPN12, and RPN15), containing the PCI (proteasome-CSN [COP9 signalosome]-eIF3 [eukaryotic translation initiation factor 3]) domains.[1,31–34] Whereas the base acts as a reverse chaperone, unfolding and translocating substrate proteins into the 20S cavity, the lid ensures substrate recognition, deubiquitination, and scaffolding.[1,31,32,35,36]

All variants reported in the present case series involve *PSMD12*, which encodes PSMD12 (aka RPN5), one of the nine subunits of the 19S lid. We therefore speculated that the above functions of the 19S lid, and thereby those of the 26S proteasome, would be substantially altered in the described subjects. Experiments in fission yeast have stressed the importance of PSMD12 dosage in the regulation of proteasome 26S assembly and the maintenance of its structural integrity.[36] Moreover, in budding yeast, PSMD12 can stabilize both the proteasome and CSN.[33,37,38]

The most likely pathogenic dysfunction for the presented disorder is *PSMD12* haploinsufficiency. *PSMD12* has a very high haploinsufficiency score (HI index = 5.57%; HI index represents the predicted probability that a gene will exhibit haploinsufficiency in comparison to a large set of genes tested by DECIPHER: high-ranked genes [e.g., HI 0%–10%] are more likely to exhibit haploinsufficiency than low-ranked ones [e.g., 90%–100%]).[39] *PSMD12* is also predicted to be highly intolerant to loss-of-function (LoF)

Please cite this article in press as: Küry et al., De Novo Disruption of the Proteasome Regulatory Subunit *PSMD12* Causes a Syndromic Neurodevelopmental Disorder, The American Journal of Human Genetics (2017), http://dx.doi.org/10.1016/j.ajhg.2017.01.003

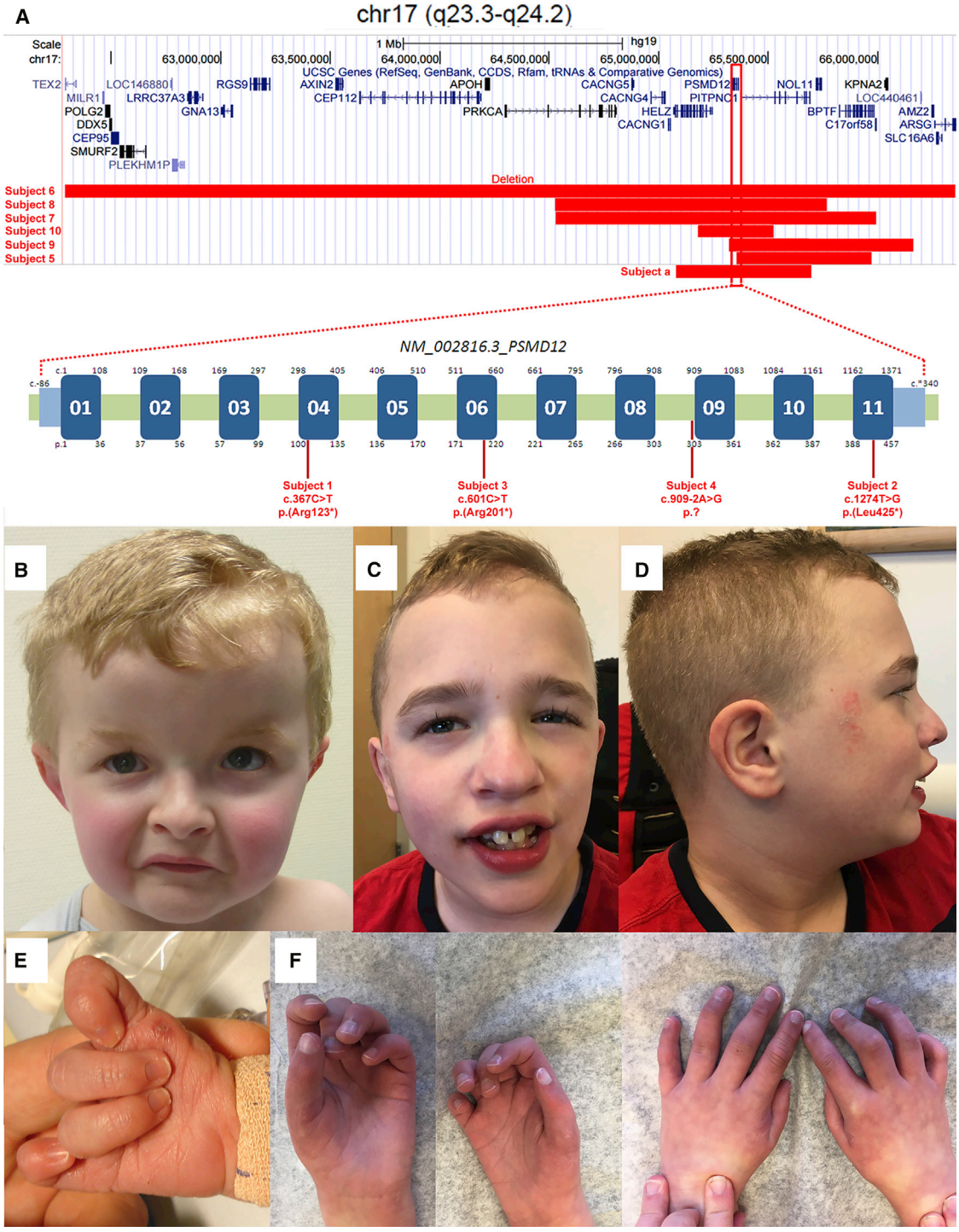

Figure 1. Mapping and Localization of the Ten *PSMD12* Variants and Morphological Anomalies in Subjects 1 and 2
A schematic representation of chromosomal region 17q24.2 shows the breakpoints of the CNV deletions encompassing *PSMD12* and localizations of the SNVs within the gene (A). Facial and hand anomalies are shown for subjects 1 (B and E) and 2 (C, D, and F). Consent for the publication of photographs was obtained for the two subjects. One additional subject with a neurodevelopmental disorder (subject a) with a smaller deletion involving *PSMD12* was tested by our CMA, albeit the detailed descriptions cannot be provided here because of privacy concerns.

mutations (probability of LoF intolerance = 1.00 with 1 observed LoF variant versus 21.5 predicted, according to the ExAC Browser).[40] Furthermore, we observed only heterozygous truncating variants or whole-gene deletions in the presented subjects. The only LoF variant reported in the ExAC Browser is predicted to alter the splicing of an in-frame *PSMD12* exon outside the functional domains of PSMD12; thus, LoF of this variant remains uncertain.

Given that the mutation c.1274T>G (p.Leu425*) in subject 2 is located in the last exon of *PSMD12*, it is predicted

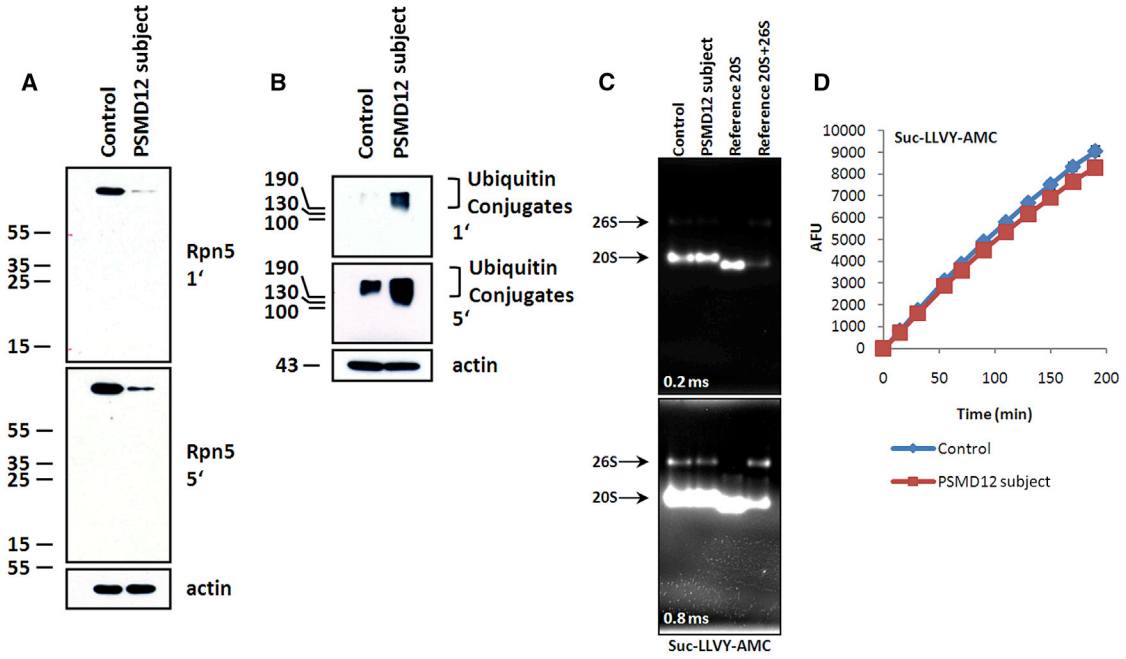

Figure 2. The c.367C>T (p.Arg123*) *PSMD12* Nonsense Mutation Leads to Decreased Levels of the Full-Length PSMD12 and Increased Accumulation of High-Molecular-Weight Ubiquitin-Modified Proteins without Altering the 20S or 26S Proteasome Complex

(A) PSMD12 (RPN5) content was determined with the H-3 monoclonal antibody (Santa Cruz Biotechnology) by western blotting. Protein extracts were prepared (as previously described[44]) from PBMCs from a healthy donor (control) and subject 1, who harbors the c.367C>T (p.Arg123*) *PSMD12* nonsense mutation. 10 μg were resolved by SDS-PAGE prior to western blotting with antibodies specific to PSMD12. For ensuring equal protein loading, the membrane was probed with a monoclonal antibody specific to β-actin (clone C4, Santa Cruz Biotechnology). Two exposure times, 1 min (above) and 2 min (below), are shown.

(B) Analysis of ubiquitin-protein conjugates in PBMCs derived from healthy (control) donors and subject 1, who harbors the c.367C>T (p.Arg123*) *PSMD12* nonsense mutation. Proteins were separated on 15% SDS gel in the presence of β-mercaptoethanol. The concentration of ubiquitin-modified proteins was determined by western blotting using an anti-ubiquitin antibody (reference no. Z0458, DAKO GmbH). For confirming equal protein loading in each lane, the membrane was probed with anti-β-actin antibody.

(C) Cell extracts from PBMCs derived from control subjects and subject 1 (who harbors the c.367C>T [p.Arg123*] nonsense mutation) were prepared with a detergent-free lysis buffer (TSDG) as previously described.[45,46] 20 μg of extract was subsequently exposed to 0.2 mM of the Suc-LLVY-AMC substrate (Bachem) and analyzed on 3%–12% gradient gels (native PAGE, Invitrogen) for chymotrypsin-like activity. Size controls consisted of 1 μg of purified spleen-derived 20S and/or 26S complex, as indicated. A gel-overlay assay for peptidase activity revealed two strongly staining bands corresponding to the 20S (670 kDa) and 26S (2 MDa) proteasome complexes in these cells. Of note, compared with the 20S reference, the 20S complex ran a little bit longer than the expected size, as evidenced by the upward shift in migration on the gel. The increased size of the 20S proteasome complex in these cells could be attributed to its association with additional interacting partners, such as PA28, which is constitutively present in immune cells.[45] Two acquisition times, 0.2 ms (above) and 0.8 ms (below), are shown.

(D) 10 μg of whole-cell lysate from PBMCs prepared from control subjects and subject 1 with TSDG buffer were incubated in a final 100 μL volume containing 0.2 mM Suc-LLVY-AMC in quadruplicate and in the presence of 2 mM ATP/DTT for various periods of time, as indicated. To determine the AMC cleavage rate reflecting the chymotrypsin-like activity, we monitored the fluorescence by using a plate reader at an excitation wavelength of 360 nm and emission wavelength of 460 nm during a period of 180 min.

to escape nonsense-mediated mRNA decay (NMD) and disrupt the PCI domain, which is essential for scaffolding involved in protein-protein interactions among the proteasome, CSN, and eIF3[41] (Figure S4). Notably, PSMD12 is integrated in the CSN and proteasome through its C-terminal portion of the PCI domain.[42] Thus, the truncated PSMD12 might fail to integrate properly with the proteasome lid.[43]

We sought to determine the functional consequences of the p.Arg123* nonsense variant in peripheral-blood mononuclear cells (PBMCs) collected from subject 1. We observed that the steady-state level of the full-length PSMD12 was significantly lower in subject 1's PBMC lysates than in those of a healthy donor (Figure 2A). The observation that the functional loss of one copy of *PSMD12* cannot be further compensated indicates that this gene is haploinsufficient, which is in line with the bioinformatic predictions and with the dramatic effect on embryogenesis associated with Psmd12 (Rpn5)-truncating variants in *Arabidopsis thaliana*.[35] Importantly, western blot analyses in subject 1's blood samples did not reveal the presence of the 122-amino-acid truncated protein with a predicted molecular mass of 13.796 kDa emerging from the *PSMD12* mutated allele. According to the manufacturer, the anti-PSMD12 antibody was raised against the first 300 amino acids of PSMD12, although the precise epitope sequence is not known. Therefore, one possible explanation for our failure to detect the truncated $PSMD12_{1–122}$ could be that the epitope recognized by the antibody is located downstream of the first 122 amino

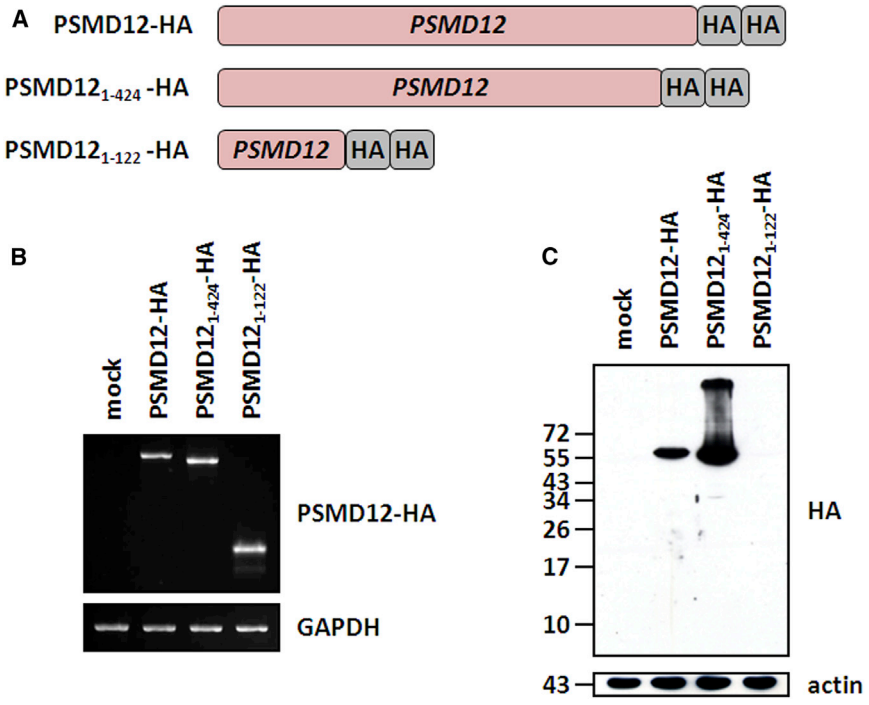

Figure 3. The c.367C>T *PSMD12* Mutant Is Efficiently Transcribed but Fails to Generate a Truncated Mature PSMD12$_{1–122}$

(A) Depiction of the PSMD12 constructs used in this study. The truncated PSMD12$_{1–424}$ and PSMD12$_{1–122}$ variants were constructed to reflect the Leu425* and Arg123* nonsense mutants, respectively. All PSMD12 constructs were cloned into the pcDNA3.1/Zeo(+) expression vector (Invitrogen) and C-terminally tagged with a double human influenza hemagglutinin (HA) epitope (GYPYDVPDYAMGGY PYDVPYAGT), as indicated.

(B) HeLa cells were cultivated in RPMI medium supplemented with 10% fetal calf serum and 1% penicillin and streptomycin (all purchased from Biochrom AG) and transfected with each of the three PSMD12 variants for 24 hr with Lipofectamin 2000 according to the manufacturer's instructions. Total RNA was extracted and analyzed by RT-PCR with forward and reverse primers specific to PSMD12 and HA, respectively. Equal loading in each lane was ensured by the amplification of GAPDH.

(C) HeLa cells transfected with the empty vector (mock) or each of our PSMD12 variants were subjected to protein extraction at 24 hr after transfection. Whole-cell extracts (20 μg) were resolved on 15% SDS-PAGE and subsequently analyzed by western blotting using anti-HA (clone 16B12, BioLegend) and anti-β-actin (loading control) antibodies, as indicated.

acids of PSMD12. Alternatively, it is also conceivable that our inability to detect the predicted PSMD12$_{1–122}$ short variant might be due to NMD and/or particular high proteolytic sensitivity and subsequent instability. To answer this question, we engineered tumor cells to produce hemagglutinin-tagged versions of both the wild-type PSMD12 and the truncated PSMD12$_{1–122}$ and PSMD12$_{1–424}$ variants emerging from the c.367T>C (p.Arg123*) and c.1274T>G (p.Leu425*) nonsense mutations, respectively (Figure 3A). As illustrated in Figures 3B and 3C, although all three constructs exhibited comparable levels of mRNA transcripts, protein levels were detected only for the wild-type and PSMD12$_{1–424}$ variant. This unambiguously indicates that our inability to detect the PSMD12$_{1–122}$ short variant was not due to NMD but rather reflects translation inefficiency and/or an increased degradation rate. Our in vitro data also show that the p.Arg123* nonsense mutant was accompanied by an increased accumulation of the high-molecular-weight ubiquitin-modified proteins (Figure 2B). This finding is consistent with the accumulation of polyubiquitinated proteins reported in yeasts with heterozygous loss of Rpn5,[36] indicating a role for PSMD12 in the maintenance of ubiquitin homeostasis. Importantly, the capacity of 26S complexes to degrade the Suc-LLVY (succinyl-Leu-Leu-Val-Tyr-amido-4-methylcoumarine) model substrate was not statistically different between the affected and control subjects (Figures 2C and 2D), indicating that both of these samples exhibit similar chymotrypsin-like activities. This finding further suggests that the elevated levels of such ubiquitin-protein conjugates in affected subjects did not result from a lower chymotrypsin activity of proteasomes. Rather, the decreased amount of PSMD12 might drive a conformational change of the 19S regulatory particle to render it deficient. In particular, PSMD12 is positioned in close proximity to the PSMD14 (RPN11) subunit,[47] which is involved in the hydrolysis of ubiquitin chains from targeted substrates before degradation by the 26S proteasome.[48] As such, the activity of PSMD14 might be affected in subjects with a downregulation of PSMD12, thereby resulting in impaired breakdown of ubiquitin-protein conjugates, which would mechanically increase the levels of polyubiquitinated substrate proteins. Alternatively, the increased accumulation of ubiquitin-modified proteins in subject 1, who carries the p.Arg123* nonsense variant, might also reflect a decreased accessibility of these substrates to the 26S proteasome through decreased amounts of incorporated RPN10 and RPN13.

Because the individuals with the *PSMD12* nonsense variants presented with central nervous system, renal, and craniofacial pathologies, we next sought to determine the function of PSMD12 during brain, kidney, and craniofacial development by utilizing the zebrafish embryo as an in vivo model. Considering the presence of disrupting mutations, we decided to use CRISPR/Cas9 technology to generate a mutant for the zebrafish ortholog of *PSMD12*. Using reciprocal BLAST, we identified a single zebrafish *PSMD12* ortholog (GenBank: NM_201578 and NP_963872) with 86% similarity and designed short guide RNA (sgRNA) targeting exon 3 of *psmd12* (Figure S5).

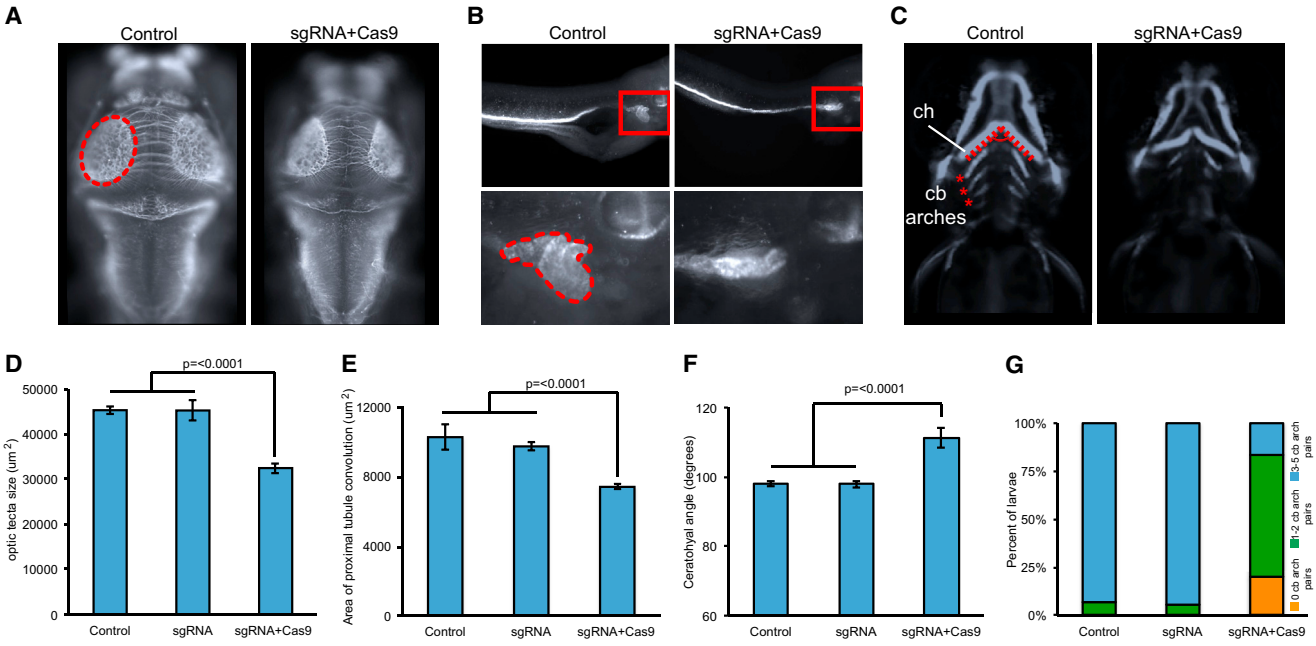

Figure 4. *psmd12* CRISPR/Cas9 Mutants Exhibit Microcephaly, Renal Tubular Atrophy, and Aberrant Rostrocaudal Patterning of the Branchial Arches in Zebrafish Larvae

(A) Representative dorsal images of 3 dpf zebrafish larvae stained with anti-acetylated tubulin show a reduction of the optic tecta (dotted oval) in F0 mutants.

(B) Representative lateral images of 4-day-old zebrafish larvae stained with anti-Na^+/K^+ ATPase alpha-1 subunit show a reduction in the convolution of the pronephric tubule (zoomed in and bordered with dotted shape in the lower panel) in F0 mutants.

(C) Representative ventral views of *-1.4col1a1:egfp* F0 mutant larvae imaged live at 3 dpf show an increase in the ceratohyal angle (ch, dotted line) and a reduction in pairs of bronchial arches (asterisks) in F0 mutants. cb, ceratobranchial.

(D) Size quantification of the optic tecta in F0 mutants targeted with CRISPR sgRNA ($p \leq 0.0001$ versus control, n = 30–50 larvae/batch, repeated).

(E) Quantification of the area of pronephric tubule convolution in F0 mutants targeted with sgRNA ($p \leq 0.0001$, n = 30–47 larvae/batch, repeated).

(F) Quantification of the ceratohyal angle in F0 mutants targeted with sgRNA ($p \leq 0.0001$, n = 32–44 larvae/batch, repeated).

(G) Categorization of F0 mutants based on pairs of ceratobranchial arches (n = 32–44 larvae/batch, repeated and observed with similar results).

Error bars represent the SEM.

CRISPR guide RNA was designed with ChopChop software (see guide sequences in Table S6) and synthesized with the GeneArt Precision gRNA Synthesis Kit (Invitrogen) according to the manufacturer's instructions. In brief, we mixed the forward and reverse target oligonucleotides, the Tracr fragment, and T7 primer mix with 2× Phusion High-Fidelity PCR Master Mix (Invitrogen) and then amplified and ran them on a 1% agarose gel to ensure the quality and appropriate size of the resulting CRISPR guide DNA template. We synthesized guide RNA by in vitro transcription with the TranscriptAid Enzyme Mix (Invitrogen) by incubating it at 37°C for 2 hr. After treatment with DNase I, the guide RNA was purified with the GeneArt gRNA Clean-Up Kit (Invitrogen). For CRISPR/Cas9-based genome editing, 100 pg of CRISPR guide RNA and 200 pg of Cas9 (GeneArt Platinum Cas9 Nuclease, Invitrogen) were injected into 1-cell-stage zebrafish embryos. The CRISPR/Cas9 efficiency was assessed as previously described.[49] In brief, DNA from each 2 day post fertilization (dpf) F0 embryo was extracted by proteinase K digestion (Life technologies, AM2548). The CRISPR-targeted region was amplified by PCR. We then denatured and slowly reannealed the PCR products to facilitate the formation of heteroduplexes (denaturing at 95°C for 5 min, ramped down to 85°C at −1°C/s and then to 25°C at −0.1°C/s). Heteroduplexes were detected on 15% polyacrylamide gel electrophoresis 23 (n = 6 F0 embryos tested/condition). Then, we cloned and sequenced PCR amplicons to estimate the mosaicism. Ultimately, we observed ≈90% mosaicism.

Given the presence of microcephaly in most of our subjects, we next measured the size of the optic tecta as a readout for head size[50] of the F0 *psmd12* zebrafish mutants. Standard whole-mount zebrafish immunostaining was performed on CRISPR experiments as previously described.[49,50] To visualize the axonal tracts in the brain, including the optic tecta and the cerebellum, we stained 3 dpf mutant and control embryos with an anti-acetylated tubulin primary antibody (T7451, mouse, Sigma-Aldrich; 1:1,000 dilution) and the Alexa Fluor goat anti-mouse IgG (A21207, Invitrogen; 1:500 dilution) as a secondary antibody.[50] We observed that the size of the optic tecta was significantly smaller in CRISPR F0 mutants than in the control larvae ($p \leq 0.0001$, n = 30–50 larvae/batch, repeated; Figures 4A and 4D).

In addition, we assessed whether *psmd12* was also required for renal development by quantifying the area of proximal tubule convolution in 4 dpf F0 *psmd12* mutants stained with an anti-Na^+/K+ ATPase alpha-1 subunit primary antibody (α6F, DSHB; 1:20 dilution) and Alexa Fluor rabbit anti-mouse IgG secondary antibody (Invitrogen; 1:500 dilution). Compared to controls, which showed properly convoluted tubules, mutant zebrafish embryos displayed qualitative defects of the proximal tubule, including absent, reduced, or v-shaped tubules. Using ImageJ software, we then measured the area of the renal tubules in both mutants and controls and observed that the area of the proximal convolution was significantly smaller in F0 mutants ($p \leq 0.0001$, n = 30–47 larvae/batch, repeated) than in controls (Figures 4B and 4E). We did not observe any larvae with a unilateral or bilateral absence of kidneys.

It has been previously shown that zebrafish models of mispatterned craniofacial cartilage reflect craniofacial abnormalities in humans.[51–53] Finally, to assess the role of *psmd12* in craniofacial development, we therefore injected CRISPR sgRNA into the *-1.4col1a1:egfp* transgenic line embryos at the 1-cell stage. *-1.4col1a1:egfp* demonstrates GFP signal in cartilages. This transgenic line contains a 1.4 kb proximal promoter fragment of Col1a1 inserted upstream of Egfp.[54] For imaging, 3 dpf larvae were positioned and imaged live with the Vertebrate Automated Screening Technology platform (version 1.2.2.8, Union Biometrica) in a manner similar to previously described methods.[53,55] We assessed craniofacial patterning by either measuring the angle of the ceratohyal cartilage at 3 dpf or by counting the number of ceratobranchial arch pairs at 3 dpf. We were then able to quantify two types of craniofacial abnormalities from GFP-positive cells in *-1.4col1a1:egfp* CRISPR F0 mutants. First, we observed a significantly broadened angle of the ceratohyal in F0 mutants ($p \leq 0.0001$, n = 32–44 larvae/batch, repeated; Figures 4C and 4F). Second, we observed a significant delay in rostrocaudal ceratobranchial (cb) arch patterning; F0 mutants showed a reduced number of cb pairs (Figures 4C and 4G).

Taken together, our data indicate that *PSMD12* plays an important role during brain, kidney, and craniofacial development and that its LoF leads to defects that are reminiscent of the phenotypes observed in our subject cohort.

The high expression of *PSMD12* in the frontal cortex (Figures S6–S8) is consistent with the main neurological component in the neurodevelopmental syndrome presented here. In support of this notion, CNV deletions of *PSMD12* were reported in two independent investigations on subjects with ID, truncal obesity, and psychiatric symptoms.[56,57] In the first study, three subjects with a complete deletion of *PSMD12* had conductive hearing loss and feeding difficulties during infancy in addition to ID.[57] In the second study, the subject with a large deletion including *PSMD12* exhibited global DD associated with a cardiac defect, feeding difficulties, and pulmonary infection,[56] clinical findings consistent with those reported in our study.

Thus far, two other genes encoding subunits of the proteasome 26S have been proposed to be associated with syndromic ID. The first gene, *PSMD14* (MIM: 607173), encodes the deubiquitinating enzyme PSMD14 (RPN11)[47,58] and was included in the 2q24.2 deletion harboring two other genes: *TBR1* (MIM: 604616), whose LoF mutations are associated with autism,[59] and *TANK* (MIM: 604834), identified in an individual with ID and short stature.[60] In a subject with a balanced complex chromosomal aberration (reciprocal translocation and paracentric inversion), *PSMD14* was considered a strong neurodevelopmental candidate gene.[61] As mentioned above, PSMD12 would need to directly interact with PSMD14 to acquire its active enzymatic conformation.[47,62] The second gene, *PSMA7*, encodes an alpha subunit of the 20S core complex. A de novo heterozygous likely pathogenic variant was found in a subject with severe ID, premature baldness, retrognathia, mild kyphosis, hirsutism, and short toes.[63]

Interestingly, PSMD12 is predicted to have direct interactions with other proteins of the UPS signaling pathway: UBE3A, UBE3B, HUWE1, USP7, and USP9X, whose dysfunction is associated with ID (Figure S9).

In conclusion, we describe a neurodevelopmental disorder caused by de novo heterozygous inactivating point mutations or CNV deletions of *PSMD12*. Future studies will attempt to unravel the impact of PSMD12 downregulation on the incorporation efficiency of other subunits into the 19S regulatory particle. These investigations would represent initial steps toward determining how proteome remodeling caused by LoF *PSMD12* variants can lead to ID, congenital malformations, and other clinical features of this neurodevelopmental syndrome.

Accession Numbers

PSMD12 sequence variants c.367C>T (p.Arg123*), c.1274T>G (p.Leu425*), c.601C>T (p.Arg201*), and c.909−2A>G (p.?) have been deposited in the Leiden Open Variation Database under accession numbers LOVD: 0000132255, 0000132256, 0000132257, and 0000132258, respectively.

Supplemental Data

Supplemental Data include a Supplemental Note, ten figures, and six tables and can be found with this article online at http://dx.doi.org/10.1016/j.ajhg.2017.01.003.

Acknowledgments

We would like to thank all families for participating in this study. We acknowledge HUGODIMS (a Western France exome-based trio-approach project to identify genes involved in intellectual disability); funding for HUGODIMS (subject 1) is supported by a grant from the French Ministry of Health and from the Health Regional Agency from Poitou-Charentes (HUGODIMS, 2013, RC14_0107). We thank Dr. Frédérique Allaire from the Health Regional Agency of Poitou-Charentes for supporting this project. We thank Léa Ferrand and Emilie Le Blanc for grant and data management. We acknowledge GEM HUGO (Western France Network

of Medical Genetics and Genomics). We are most grateful to the Nantes Genomics core facility (Biogenouest Genomics) for its technical support and for performing exome sequencing for subject 1 and his parents. This work was supported in part by grant U54HG006542 from the US National Human Genome Research Institute and National Heart, Lung, and Blood Institute to the Baylor Hopkins Center for Mendelian Genomics. This study made use of data generated by the DECIPHER community. A full list of centers who contributed to data generation is available at http://decipher.sanger.ac.uk and via email at decipher@sanger.ac.uk. Funding for the project was provided by the Wellcome Trust. M.T.C, K.G.M, and K.R. are employees of GeneDx.

Received: November 3, 2016
Accepted: January 4, 2017
Published: January 26, 2017

Web Resources

1000 Genomes, http://www.1000genomes.org/
ChopChop software, https://chopchop.rc.fas.harvard.edu/
Database of Genomic Variants, http://dgv.tcag.ca/dgv/app/home/
DECIPHER, https://decipher.sanger.ac.uk/
dbSNP, http://www.ncbi.nlm.nih.gov/projects/SNP/
GeneMatcher, https://genematcher.org/
ExAC Browser, http://exac.broadinstitute.org/
GenBank, http://www.ncbi.nlm.nih.gov/genbank/
Leiden Open Variation Database, http://www.lovd.nl/
NHLBI Exome Sequencing Project (ESP) Exome Variant Server, http://evs.gs.washington.edu/EVS/
OMIM, http://www.omim.org/
PLINK, http://pngu.mgh.harvard.edu/~purcell/plink/
The Human Protein Atlas, http://www.proteinatlas.org/
UCSC Genome Browser, http://genome.ucsc.edu

References

1. Sullivan, J.A., Shirasu, K., and Deng, X.W. (2003). The diverse roles of ubiquitin and the 26S proteasome in the life of plants. Nat. Rev. Genet. *4*, 948–958.
2. Goldberg, A.L. (2003). Protein degradation and protection against misfolded or damaged proteins. Nature *426*, 895–899.
3. Hershko, A., and Ciechanover, A. (1998). The ubiquitin system. Annu. Rev. Biochem. *67*, 425–479.
4. Finley, D. (2009). Recognition and processing of ubiquitin-protein conjugates by the proteasome. Annu. Rev. Biochem. *78*, 477–513.
5. Murata, S., Yashiroda, H., and Tanaka, K. (2009). Molecular mechanisms of proteasome assembly. Nat. Rev. Mol. Cell Biol. *10*, 104–115.
6. Voges, D., Zwickl, P., and Baumeister, W. (1999). The 26S proteasome: a molecular machine designed for controlled proteolysis. Annu. Rev. Biochem. *68*, 1015–1068.
7. Hamilton, A.M., and Zito, K. (2013). Breaking it down: the ubiquitin proteasome system in neuronal morphogenesis. Neural Plast. *2013*, 196848.
8. Tai, H.C., and Schuman, E.M. (2008). Ubiquitin, the proteasome and protein degradation in neuronal function and dysfunction. Nat. Rev. Neurosci. *9*, 826–838.
9. Cajigas, I.J., Will, T., and Schuman, E.M. (2010). Protein homeostasis and synaptic plasticity. EMBO J. *29*, 2746–2752.
10. Hegde, A.N., Haynes, K.A., Bach, S.V., and Beckelman, B.C. (2014). Local ubiquitin-proteasome-mediated proteolysis and long-term synaptic plasticity. Front. Mol. Neurosci. *7*, 96.
11. Acconcia, F., Sigismund, S., and Polo, S. (2009). Ubiquitin in trafficking: the network at work. Exp. Cell Res. *315*, 1610–1618.
12. Schwarz, L.A., and Patrick, G.N. (2012). Ubiquitin-dependent endocytosis, trafficking and turnover of neuronal membrane proteins. Mol. Cell. Neurosci. *49*, 387–393.
13. Dantuma, N.P., and Bott, L.C. (2014). The ubiquitin-proteasome system in neurodegenerative diseases: precipitating factor, yet part of the solution. Front. Mol. Neurosci. *7*, 70.
14. Fecto, F., Esengul, Y.T., and Siddique, T. (2014). Protein recycling pathways in neurodegenerative diseases. Alzheimers Res. Ther. *6*, 13.
15. Kishino, T., Lalande, M., and Wagstaff, J. (1997). UBE3A/E6-AP mutations cause Angelman syndrome. Nat. Genet. *15*, 70–73.
16. Basel-Vanagaite, L., Dallapiccola, B., Ramirez-Solis, R., Segref, A., Thiele, H., Edwards, A., Arends, M.J., Miró, X., White, J.K., Désir, J., et al. (2012). Deficiency for the ubiquitin ligase UBE3B in a blepharophimosis-ptosis-intellectual-disability syndrome. Am. J. Hum. Genet. *91*, 998–1010.
17. Froyen, G., Corbett, M., Vandewalle, J., Jarvela, I., Lawrence, O., Meldrum, C., Bauters, M., Govaerts, K., Vandeleur, L., Van Esch, H., et al. (2008). Submicroscopic duplications of the hydroxysteroid dehydrogenase HSD17B10 and the E3 ubiquitin ligase HUWE1 are associated with mental retardation. Am. J. Hum. Genet. *82*, 432–443.
18. Hao, Y.H., Fountain, M.D., Jr., Fon Tacer, K., Xia, F., Bi, W., Kang, S.H., Patel, A., Rosenfeld, J.A., Le Caignec, C., Isidor, B., et al. (2015). USP7 Acts as a Molecular Rheostat to Promote WASH-Dependent Endosomal Protein Recycling and Is Mutated in a Human Neurodevelopmental Disorder. Mol. Cell *59*, 956–969.
19. Homan, C.C., Kumar, R., Nguyen, L.S., Haan, E., Raymond, F.L., Abidi, F., Raynaud, M., Schwartz, C.E., Wood, S.A., Gecz, J., and Jolly, L.A. (2014). Mutations in USP9X are associated with X-linked intellectual disability and disrupt neuronal cell migration and growth. Am. J. Hum. Genet. *94*, 470–478.
20. Sobreira, N., Schiettecatte, F., Valle, D., and Hamosh, A. (2015). GeneMatcher: a matching tool for connecting investigators with an interest in the same gene. Hum. Mutat. *36*, 928–930.
21. Firth, H.V., Richards, S.M., Bevan, A.P., Clayton, S., Corpas, M., Rajan, D., Van Vooren, S., Moreau, Y., Pettett, R.M., and Carter, N.P. (2009). DECIPHER: Database of Chromosomal Imbalance and Phenotype in Humans Using Ensembl Resources. Am. J. Hum. Genet. *84*, 524–533.
22. Isidor, B., Küry, S., Rosenfeld, J.A., Besnard, T., Schmitt, S., Joss, S., Davies, S.J., Lebel, R.R., Henderson, A., Schaaf, C.P., et al. (2016). De Novo Truncating Mutations in the Kinetochore-Microtubules Attachment Gene CHAMP1 Cause Syndromic Intellectual Disability. Hum. Mutat. *37*, 354–358.
23. Retterer, K., Juusola, J., Cho, M.T., Vitazka, P., Millan, F., Gibellini, F., Vertino-Bell, A., Smaoui, N., Neidich, J., Monaghan, K.G., et al. (2016). Clinical application of whole-exome sequencing across clinical indications. Genet. Med. *18*, 696–704.
24. Iossifov, I., O'Roak, B.J., Sanders, S.J., Ronemus, M., Krumm, N., Levy, D., Stessman, H.A., Witherspoon, K.T., Vives, L., Patterson, K.E., et al. (2014). The contribution of de novo coding mutations to autism spectrum disorder. Nature *515*, 216–221.

25. Bainbridge, M.N., Wang, M., Wu, Y., Newsham, I., Muzny, D.M., Jefferies, J.L., Albert, T.J., Burgess, D.L., and Gibbs, R.A. (2011). Targeted enrichment beyond the consensus coding DNA sequence exome reveals exons with higher variant densities. Genome Biol. *12*, R68.
26. Yang, Y., Muzny, D.M., Reid, J.G., Bainbridge, M.N., Willis, A., Ward, P.A., Braxton, A., Beuten, J., Xia, F., Niu, Z., et al. (2013). Clinical whole-exome sequencing for the diagnosis of mendelian disorders. N. Engl. J. Med. *369*, 1502–1511.
27. Boone, P.M., Bacino, C.A., Shaw, C.A., Eng, P.A., Hixson, P.M., Pursley, A.N., Kang, S.H., Yang, Y., Wiszniewska, J., Nowakowska, B.A., et al. (2010). Detection of clinically relevant exonic copy-number changes by array CGH. Hum. Mutat. *31*, 1326–1342.
28. Wiszniewska, J., Bi, W., Shaw, C., Stankiewicz, P., Kang, S.H., Pursley, A.N., Lalani, S., Hixson, P., Gambin, T., Tsai, C.H., et al. (2014). Combined array CGH plus SNP genome analyses in a single assay for optimized clinical testing. Eur. J. Hum. Genet. *22*, 79–87.
29. MacDonald, J.R., Ziman, R., Yuen, R.K., Feuk, L., and Scherer, S.W. (2014). The Database of Genomic Variants: a curated collection of structural variation in the human genome. Nucleic Acids Res. *42*, D986–D992.
30. Gomes, A.V. (2013). Genetics of proteasome diseases. Scientifica (Cairo) *2013*, 637629.
31. Bhattacharyya, S., Yu, H., Mim, C., and Matouschek, A. (2014). Regulated protein turnover: snapshots of the proteasome in action. Nat. Rev. Mol. Cell Biol. *15*, 122–133.
32. Sharon, M., Taverner, T., Ambroggio, X.I., Deshaies, R.J., and Robinson, C.V. (2006). Structural organization of the 19S proteasome lid: insights from MS of intact complexes. PLoS Biol. *4*, e267.
33. Glickman, M.H., Rubin, D.M., Coux, O., Wefes, I., Pfeifer, G., Cjeka, Z., Baumeister, W., Fried, V.A., and Finley, D. (1998). A subcomplex of the proteasome regulatory particle required for ubiquitin-conjugate degradation and related to the COP9-signalosome and eIF3. Cell *94*, 615–623.
34. Rubin, D.M., Glickman, M.H., Larsen, C.N., Dhruvakumar, S., and Finley, D. (1998). Active site mutants in the six regulatory particle ATPases reveal multiple roles for ATP in the proteasome. EMBO J. *17*, 4909–4919.
35. Book, A.J., Smalle, J., Lee, K.H., Yang, P., Walker, J.M., Casper, S., Holmes, J.H., Russo, L.A., Buzzinotti, Z.W., Jenik, P.D., and Vierstra, R.D. (2009). The RPN5 subunit of the 26s proteasome is essential for gametogenesis, sporophyte development, and complex assembly in Arabidopsis. Plant Cell *21*, 460–478.
36. Yen, H.C., Espiritu, C., and Chang, E.C. (2003). Rpn5 is a conserved proteasome subunit and required for proper proteasome localization and assembly. J. Biol. Chem. *278*, 30669–30676.
37. Collins, S.R., Miller, K.M., Maas, N.L., Roguev, A., Fillingham, J., Chu, C.S., Schuldiner, M., Gebbia, M., Recht, J., Shales, M., et al. (2007). Functional dissection of protein complexes involved in yeast chromosome biology using a genetic interaction map. Nature *446*, 806–810.
38. Maytal-Kivity, V., Pick, E., Piran, R., Hofmann, K., and Glickman, M.H. (2003). The COP9 signalosome-like complex in S. cerevisiae and links to other PCI complexes. Int. J. Biochem. Cell Biol. *35*, 706–715.
39. Huang, N., Lee, I., Marcotte, E.M., and Hurles, M.E. (2010). Characterising and predicting haploinsufficiency in the human genome. PLoS Genet. *6*, e1001154.
40. Lek, M., Karczewski, K.J., Minikel, E.V., Samocha, K.E., Banks, E., Fennell, T., O'Donnell-Luria, A.H., Ware, J.S., Hill, A.J., Cummings, B.B., et al.; Exome Aggregation Consortium (2016). Analysis of protein-coding genetic variation in 60,706 humans. Nature *536*, 285–291.
41. Kim, H.M., Yu, Y., and Cheng, Y. (2011). Structure characterization of the 26S proteasome. Biochim. Biophys. Acta *1809*, 67–79.
42. Yu, Z., Kleifeld, O., Lande-Atir, A., Bsoul, M., Kleiman, M., Krutauz, D., Book, A., Vierstra, R.D., Hofmann, K., Reis, N., et al. (2011). Dual function of Rpn5 in two PCI complexes, the 26S proteasome and COP9 signalosome. Mol. Biol. Cell *22*, 911–920.
43. Peters, L.Z., Karmon, O., David-Kadoch, G., Hazan, R., Yu, T., Glickman, M.H., and Ben-Aroya, S. (2015). The protein quality control machinery regulates its misassembled proteasome subunits. PLoS Genet. *11*, e1005178.
44. Ebstein, F., Lehmann, A., and Kloetzel, P.M. (2012). The FAT10- and ubiquitin-dependent degradation machineries exhibit common and distinct requirements for MHC class I antigen presentation. Cell. Mol. Life Sci. *69*, 2443–2454.
45. Bochmann, I., Ebstein, F., Lehmann, A., Wohlschlaeger, J., Sixt, S.U., Kloetzel, P.M., and Dahlmann, B. (2014). T lymphocytes export proteasomes by way of microparticles: a possible mechanism for generation of extracellular proteasomes. J. Cell. Mol. Med. *18*, 59–68.
46. Seifert, U., Bialy, L.P., Ebstein, F., Bech-Otschir, D., Voigt, A., Schröter, F., Prozorovski, T., Lange, N., Steffen, J., Rieger, M., et al. (2010). Immunoproteasomes preserve protein homeostasis upon interferon-induced oxidative stress. Cell *142*, 613–624.
47. Dambacher, C.M., Worden, E.J., Herzik, M.A., Martin, A., and Lander, G.C. (2016). Atomic structure of the 26S proteasome lid reveals the mechanism of deubiquitinase inhibition. eLife *5*, e13027.
48. Boehringer, J., Riedinger, C., Paraskevopoulos, K., Johnson, E.O., Lowe, E.D., Khoudian, C., Smith, D., Noble, M.E., Gordon, C., and Endicott, J.A. (2012). Structural and functional characterization of Rpn12 identifies residues required for Rpn10 proteasome incorporation. Biochem. J. *448*, 55–65.
49. Bolar, N.A., Golzio, C., Živná, M., Hayot, G., Van Hemelrijk, C., Schepers, D., Vandeweyer, G., Hoischen, A., Huyghe, J.R., Raes, A., et al. (2016). Heterozygous Loss-of-Function SEC61A1 Mutations Cause Autosomal-Dominant Tubulo-Interstitial and Glomerulocystic Kidney Disease with Anemia. Am. J. Hum. Genet. *99*, 174–187.
50. Borck, G., Hög, F., Dentici, M.L., Tan, P.L., Sowada, N., Medeira, A., Gueneau, L., Thiele, H., Kousi, M., Lepri, F., et al. (2015). BRF1 mutations alter RNA polymerase III-dependent transcription and cause neurodevelopmental anomalies. Genome Res. *25*, 155–166.
51. Dauber, A., Golzio, C., Guenot, C., Jodelka, F.M., Kibaek, M., Kjaergaard, S., Leheup, B., Martinet, D., Nowaczyk, M.J., Rosenfeld, J.A., et al. (2013). SCRIB and PUF60 are primary drivers of the multisystemic phenotypes of the 8q24.3 copy-number variant. Am. J. Hum. Genet. *93*, 798–811.
52. Gordon, C.T., Weaver, K.N., Zechi-Ceide, R.M., Madsen, E.C., Tavares, A.L., Oufadem, M., Kurihara, Y., Adameyko, I., Picard, A., Breton, S., et al. (2015). Mutations in the endothelin receptor type A cause mandibulofacial dysostosis with alopecia. Am. J. Hum. Genet. *96*, 519–531.
53. Isrie, M., Breuss, M., Tian, G., Hansen, A.H., Cristofoli, F., Morandell, J., Kupchinsky, Z.A., Sifrim, A., Rodriguez-Rodriguez,

C.M., Dapena, E.P., et al. (2015). Mutations in Either TUBB or MAPRE2 Cause Circumferential Skin Creases Kunze Type. Am. J. Hum. Genet. *97*, 790–800.

54. Kague, E., Gallagher, M., Burke, S., Parsons, M., Franz-Odendaal, T., and Fisher, S. (2012). Skeletogenic fate of zebrafish cranial and trunk neural crest. PLoS ONE *7*, e47394.
55. Pardo-Martin, C., Allalou, A., Medina, J., Eimon, P.M., Wählby, C., and Fatih Yanik, M. (2013). High-throughput hyperdimensional vertebrate phenotyping. Nat. Commun. *4*, 1467.
56. Bartnik, M., Nowakowska, B., Derwińska, K., Wiśniowiecka-Kowalnik, B., Kędzior, M., Bernaciak, J., Ziemkiewicz, K., Gambin, T., Sykulski, M., Bezniakow, N., et al. (2014). Application of array comparative genomic hybridization in 256 patients with developmental delay or intellectual disability. J. Appl. Genet. *55*, 125–144.
57. Vergult, S., Dauber, A., Delle Chiaie, B., Van Oudenhove, E., Simon, M., Rihani, A., Loeys, B., Hirschhorn, J., Pfotenhauer, J., Phillips, J.A., 3rd., et al. (2012). 17q24.2 microdeletions: a new syndromal entity with intellectual disability, truncal obesity, mood swings and hallucinations. Eur. J. Hum. Genet. *20*, 534–539.
58. Cooper, E.M., Cutcliffe, C., Kristiansen, T.Z., Pandey, A., Pickart, C.M., and Cohen, R.E. (2009). K63-specific deubiquitination by two JAMM/MPN+ complexes: BRISC-associated Brcc36 and proteasomal Poh1. EMBO J. *28*, 621–631.
59. Notwell, J.H., Heavner, W.E., Darbandi, S.F., Katzman, S., McKenna, W.L., Ortiz-Londono, C.F., Tastad, D., Eckler, M.J., Rubenstein, J.L., McConnell, S.K., et al. (2016). TBR1 regulates autism risk genes in the developing neocortex. Genome Res. *26*, 1013–1022.
60. Burrage, L.C., Eble, T.N., Hixson, P.M., Roney, E.K., Cheung, S.W., and Franco, L.M. (2013). A mosaic 2q24.2 deletion narrows the critical region to a 0.4 Mb interval that includes TBR1, TANK, and PSMD14. Am. J. Med. Genet. A. *161A*, 841–844.
61. Blake, J., Riddell, A., Theiss, S., Gonzalez, A.P., Haase, B., Jauch, A., Janssen, J.W., Ibberson, D., Pavlinic, D., Moog, U., et al. (2014). Sequencing of a patient with balanced chromosome abnormalities and neurodevelopmental disease identifies disruption of multiple high risk loci by structural variation. PLoS ONE *9*, e90894.
62. Verma, R., Aravind, L., Oania, R., McDonald, W.H., Yates, J.R., 3rd, Koonin, E.V., and Deshaies, R.J. (2002). Role of Rpn11 metalloprotease in deubiquitination and degradation by the 26S proteasome. Science *298*, 611–615.
63. de Ligt, J., Willemsen, M.H., van Bon, B.W., Kleefstra, T., Yntema, H.G., Kroes, T., Vulto-van Silfhout, A.T., Koolen, D.A., de Vries, P., Gilissen, C., et al. (2012). Diagnostic exome sequencing in persons with severe intellectual disability. N. Engl. J. Med. *367*, 1921–1929.